Persistent Epstein-Barr virus infection of epithelial cells leads to APOBEC3C expression and induces mitochondrial DNA mutations

Aung Phyo Wai[1], Richardo Timmy[1,2], Kousho Wakae[3], Shunpei Okada[1], Masamichi Muramatsu[4], Hironori Yoshiyama[1*], and Hisashi Iizasa[1*]

[1]Department of Microbiology, Faculty of Medicine, Shimane University, 89-1 Enya, Izumo, Shimane, Japan; [2] Institute of Immunology, Department of Innate Immunity, University of Tübingen, Tübingen, Germany; [3] Department of Virology II, National Institute of Infectious Disease, Tokyo, Japan*; [4] Department of Infectious Disease Research, Foundation for Biomedical Research and Innovation at Kobe, Kobe, Hyogo, Japan.*

Correspondence: Address correspondence to: Prof. Dr. Hironori Yoshiyama and Dr. Hisashi Iizasa and, 89-1 Enya, Izumo, Shimane 693-8501, Japan. Email: yosiyama@med.shimane-u.ac.jp (H.Y.), iizasah@med.shimane-u.ac.jp (H.I.); TEL: +81-853-20-2149 (H.Y.), +81-853-20-2146 (H.I.), FAX: +81-853-20-2147 (H.I., H.Y.).

Abbreviations

APOBEC3: Apolipoprotein B mRNA editing enzyme, catalytic polypeptide-like 3, BART: *Bam*HI-rightward transcript, B2M: beta-2-microglobulin gene, cDNA: Complementary DNA, crRNA: CRISPR RNA, C-to-U: Cytosine to uracil, CRISPR: Clustered Regularly Interspaced Short Palindromic Repeats, DAPI: 4',6-diamidino-2-phenylindole, eGFP: Enhanced green fluorescent protein, EBERs**:** EBV-encoded small RNAs, EBNA1: EBV nuclear antigen 1, EBV: Epstein-Barr virus, EBVaGC: EBV-associated gastric cancer, GAPDH: Glyceraldehyde-3-phosphate dehydrogenase, HSP: Heat shock protein, HSV-1: herpes simplex virus-1,LMP2A: Latent membrane protein 2A, mtDNA: Mitochondrial DNA, MT-tRNA: mitochondrial-tRNA, NF-κB: Nuclear factor kappa-B, PBS (-): Phosphate-buffered saline without Ca^{++} and Mg^{++}, RIPA: radioimmunoprecipitation assay, RT-qPCR: Reverse transcription-quantitative polymerase chain reaction, TFAM: transcription factor A, mitochondrial, TBST: Tris-buffered saline containing 0.1% Tween 20, 3D-PCR: Differential denaturation DNA PCR, trTRNA: tracer RNA, HRP: horse radish peroxidase.

Key wards: Epstein-Barr virus, APOBEC3C, Mitochondria, EBVaGC, D-loop

Abstract Upon infected with virus, cells increase the expression of cytidine deaminase APOBEC3 family genes. This leads to the accumulation of C-to-T mutations in the replicating viral genome, and suppresses viral propagation. On the other hand, herpesviruses including Epstein-Barr virus (EBV) express genes that counteracts APOBEC3 during lytic infection. However, since viral resistance factors are not expressed during EBV latent infection, it is unknown how APOBEC3 functions during latent infection. We observed that in gastric epithelial cells persistently infected with EBV, the expression of APOBEC3 family genes increased, C-to-T mutations in the D-loop genome of mitochondrial DNA (mtDNA) increased, and mtDNA copy number decreased. By introducing and expressing individual APOBEC3 family genes, APOBEC3C was particularly expressed in the cytoplasm, increasing C-to-T mutations in mtDNA and decreasing mtDNA copy number. Furthermore, we confirmed that APOBEC3C colocalized with mitochondria in EBV-infected cells. Expression of the EBV latent gene LMP2A increased APOBEC3C expression. Conversely, APOBEC3C expression was reduced in LMP2A-deficient EBV-infected cells compared to wild-type EBV-infected cells. These results indicate that persistent infection of EBV in gastric epithelial cells reduces the number of mitochondria through mtDNA mutations induced by APOBEC3C expression.

Introduction

Epstein-Barr virus (EBV) infects lymphocytes and epithelial cells and is associated with the formation of tumors such as gastric cancer and nasopharyngeal cancer (Burke AP et al., *Mod Pathol,* 1990, Imai S et al., *Proc Natl Acad Sci U S A*, 1994, Henle W et al., *Science*, 1970). These EBV-associated tumors arise from cells latently infected with EBV, and persistent expression of viral genes promotes tumor formation (Iizasa H et al., *Viruses*, 2012). In tumor cells of EBV-associated gastric cancer (EBVaGC), which accounts for approximately 10% of all gastric cancers, EBV shows type I latent infection, and only a few EBV genes are expressed, including EBV nuclear antigen 1 (EBNA1), latent membrane protein 2A (LMP2A), EBV-encoded small RNAs (EBERs), and *Bam*HI-rightward transcript (BART). Moreover, EBVaGC does not express LMP1, which induces activation of nuclear factor kappa-B (NF-κB) and promotes tumorigenesis (Iizasa H et al., *Viruses*, 2012). Furthermore, EBVaGC does not show p53 mutations or driver gene abnormalities such as Myc, which are seen in Burkitt lymphoma (Cancer Genome Atlas Research Network, *Nature*, 2014). Because there are few gene mutations in EBVaGC tumor cells and the number of expressed viral latent infection genes is limited, the details of the molecular mechanism by which EBV infection promotes tumorigenesis in gastric epithelial cells remain unclear.

Apolipoprotein B mRNA Editing Enzyme, Catalytic Polypeptide-Like 3 (APOBEC3) proteins are cytidine deaminases that convert cytosine to uracil (C-to-U mutation) in host and viral genes

(Swanton C et al., *Cancer Discov*, 2015). The APOBEC3 gene group was first reported to be upregulated as a defense factor for host cells against infection by viruses, particularly retroviruses, and to introduce genetic mutations into viral genomes (Harris RS et al., *Cell*, 2003). APOBEC3 is also known to cause C-to-T mutations in the genomes of DNA viruses such as EBV, hepatitis B virus, and human papillomavirus, and inhibits viral proliferation (Suspène R et a., *Proc Natl Acad Sci U S A*, 2005, Vartanian JP et al., *Science*, 2008, Wang Z et al., *J Virol*, 2014). In response to the APOBEC3 family's assault on the viral genome, EBV uses the viral protein BORF2 during lytic infection to facilitate the export of APOBEC3B from the nucleus (Cheng AZ et al., *Nat Microbiol*, 2018).

In addition, it has been suggested that APOBEC3 may introduce mutations not only into the viral genome but also into the host genome and mitochondrial DNA (mtDNA) (Burns MB et al., *Nature*, 2013, Suspène R et al., *Proc Natl Acad Sci U S A*, 2005). Although the expression of the APOBEC3 family is mostly induced by type I interferon, APOBEC3C is not induced by interferon (Refsland EW et al., *Nucleic Acids Res*, 2010). Moreover, the tightly chromatinized EBV genomes in latent infection provides protection against APOBEC3 enzymes, which typically target more accessible, single-stranded DNA. The tethering of EBV episomes to host chromosomes might also shield the viral genome from APOBEC3 enzymes during latency

because it mimics host chromatin (Coursey TL et al., *Annu Rev Virol*, 2019, Kanda T et al., *J Biol Chem*, 2013).

It has been reported that the morphology of mitochondria changes from fused to fissile in the LMP2A-expressing AGS clone 5 and EBVaGC-derived SNU719 cell line compared with gastric epithelial cell line AGS (Pal AD et al., *Carcinogenesis*, 2014). In addition, it has been reported that the expression level of mitochondria-related genes is reduced in EBVaGC (Wang Z et al., *Cancer Cell Int*, 2021). On the other hand, it is known that mtDNA is mutated in many cancer cells, and mtDNA mutations lead to reduced oxygen consumption and suppression of apoptosis (Shidara Y et al., *Cancer Res*, 2005). These mitochondrial disorders reduce oxidative phosphorylation in mitochondria. As a compensatory mechanism, cells upregulate the glycolytic pathway to meet their energy demands, leading to increased ATP production via glycolysis and induction of the Warburg effect, where glucose is preferentially converted to lactate even in the presence of oxygen (Wallace DC, *Nat Rev Cancer*, 2012) to allow cells to sustain ATP levels despite reduced mitochondrial function.

However, there have been no detailed investigations into mitochondrial dysfunction in EBVaGC. Here, we report that EBV infection induces the expression of the APOBEC3 family in gastric epithelial cell lines, and that APOBEC3C in particular causes severe damage to host mitochondria.

Materials and Methods

Cell Culture

Cells were cultured in RPMI-1640 (Sigma-Aldrich, St. Louis, MO) supplemented with 10% fetal bovine serum, 100 units/mL of penicillin, and 100 μg/mL of streptomycin (Nacalai, Kyoto, Japan) at 37°C in a 5% CO_2 incubator. Human gastric cancer cell lines AGS (ATCC, Manassas, VA) and MKN28 (JCRB Cell Bank, Tokyo, Japan) (Nakatani H et al., *Jpn J Cancer Res*, 1986) were used. AGS and MKN28 cells were persistently infected with EBV carrying the enhanced green fluorescent protein (eGFP) gene integrated into the encodes the viral thymidine kinase (Maruuo S et al., *J Gen Virol*, 2001). AGS cells persistently infected with LMP2A-deficient EBV (Konishi K et al., *J Gen Virol*, 2001) were also used. EBV-positive cells were selected with 700 μg/mL G418 (Promega, Madison, WI) and maintained in medium containing 500 μg/mL G418.

Reverse transcription-quantitative polymerase chain reaction (RT-qPCR)

Total RNA was extracted from cells using ISOGEN (FUJIFILM Wako, Osaka, Japan) according to the manufacturer's protocol. RNA was treated with DNaseI (DNaseI AmpGrade, Thermo Fisher Scientific, Waltham, MA) and then synthesized into complementary DNA (cDNA) using Superscript III transcriptase (Thermo Fisher Scientific) and random hexamer (Promega). RT-qPCR was performed using SsoAdvanced™ Universal SYBR Green Supermix

(Bio-Rad, Hercules, CA) and specific primers (**Table 1**) using the CFX connect real-time PCR system (Bio-Rad) (Kitamura K et al., *PLoS Pathog*, 2013). All primers were synthesized by Integrated DNA technologies (IDT, Skokie, IL). Glyceraldehyde-3-phosphate dehydrogenase (GAPDH) expression was used as an internal control.

Differential denaturation DNA PCR (3D-PCR)

C-to-T mutations in genomic DNA were detected by 3D-PCR as follows (Suspène R et al., *Proc Natl Acad Sci U S A*, 2005). First, genomic DNA from cultured cells was extracted using the GenElute Mammalian Genomic DNA kit (Sigma-Aldrich) according to the manufacturer's protocol. Next, primary PCR was performed using 500 ng of genomic DNA as a template with specific primers (**Table 2**) and TaKaRa LA Taq Hot Start Version (TAKARA BIO, Shiga, Japan). Then, secondary PCR was performed using 0.1 μL of the primary PCR product as a template with specific primers (**Table 2**) and KAPA2G Fast HotStart ReadyMix (KAPA Biosystem, Wilmington, MA). The conditions for each PCR are shown in **Table 3**. The secondary PCR products were separated by electrophoresis using 1% agarose gel. We also purified the secondary PCR products using a QIAEX II gel extraction kit (QIAGEN, Hilden, Germany) according to the manufacturer's protocol, cloned them into pGEM-T Easy Vector (Promega), and determined the DNA sequence.

Immunostaining

Cells were cultured overnight on sterile poly-L-lysine-coated coverslips (13 mm ø, Matsunami, Osaka, Japan) in a CO_2 incubator to allow attachment. The attached cells were then washed once with phosphate-buffered saline without Ca^{++} and Mg^{++} (PBS (-)) and fixed using Mildform 10N (FUJIFILM Wako). The fixed cells were treated at room temperature with PBS (-) containing 0.5% Triton X-100 and then blocked at room temperature with PBST (PBS (-) with 0.1% Tween 20) containing 5% bovine serum albumin. Next, the cells were incubated with primary antibodies diluted in Can Get Signal immunostain Immunoreaction Enhancer Solution A (TOYOBO, Osaka, Japan) for 30 minutes in a humidified chamber at 37°C. The primary antibodies used were rabbit monoclonal anti-Heat Shock Protein (HSP) 60 antibody (D6F1, Cell Signaling Tech, Danvers, MA), mouse anti-transcription factor A, mitochondrial (TFAM) antibody (18G102B2E11, Biolegend, San Diego, CA), and rabbit polyclonal anti-APOBEC3C antibody (GTX102164, GeneTex, Irvine, CA). The cells treated with the primary antibodies were washed twice with PBST. Subsequently, secondary antibody reactions were performed using Alexa Fluor 568-labeled goat anti-rabbit IgG antibody (Thermo Fisher Scientific), Hilyte Fluor 647-labeled goat anti-mouse IgG antibody (Anaspec, Fremont, CA), and Alexa Fluor 568-labeled donkey anti-rabbit IgG antibody (Thermo Fisher Scientific), respectively. Each secondary antibody was

diluted in Can Get Signal immunostain Immunoreaction Enhancer Solution B. The cells treated with the secondary antibodies were washed twice with PBST. Nuclear DNA was counterstained with 4',6-diamidino-2-phenylindole (DAPI) (Wako). The stained cells were then mounted using ProLong Diamond Antifade (Thermo Fisher Scientific) and observed under a confocal microscope FV-1000D (Olympus, Tokyo, Japan).

Intensity-based co-localization analysis

For quantification of the intracellular distribution of mitochondria (TFAM) and APOBEC3C, images for more than 10 cells in three to five fields were acquired with a z-stack of approximately 20 slices at 0.2 μm intervals. Z-stack images were reconstructed with imaging software (IMARIS; OXFORD Instruments, Oxfordshire, UK). The cellSens (Evident Scientific) was used to calculate the maximal fluorescence intensity of the channels to determine the distribution of the individual fluorescence signals. Z-stack images were reconstructed and analyzed using the ImarisCo-loc module (Furuyama W et al. *Microbiol Spectr,* 2024).

Quantification of mtDNA copy number

The copy numbers of mitochondrial-tRNA (MT-tRNA) genes were measured by qPCR using DNA extracted from cultured cells as a template and a specific primer set (F: 5'-

CACCCAAGAACA GGGTTTGT-3'; R, 5'-TGGCCATGGGTATGTTGTTA-3') and Universal SYBR Green Supermix on a CFX connect real-time PCR system. The beta-2-microglobulin gene (B2M) was measured as an internal standard using a B2M-specific primer set (F, 5'-TGCTGTCTCCATGTT TGATGTATCT-3'; R, 5'-TGGCCATGGGTATGTTGTTA-3'). The mtDNA copy number per cell was calculated from the difference in Ct values between B2M and MT-tRNA derived from the human genome using the following formula: mtDNA copy number $= 2 \times 2^{(\text{Ct of } B2M - \text{Ct of MT-tRNA})}$ (Venegas V et al., *Curr Protoc Hum Genet*, 2011).

Immunoblotting

Cells were lysed using radioimmunoprecipitation assay (RIPA) buffer (Thermo Fisher Scientific) containing a protease inhibitor (cOmplete™ Mini Protease Inhibitor Cocktail, Sigma-Aldrich). Each sample was separated by electrophoresis using 12.5% SDS-polyacrylamide gel and then transferred onto a 0.2 μm PVDF membrane (Millipore, Kenilworth, NJ). After the transfer, the membranes were blocked with Tris-buffered saline containing 0.1% Tween 20 (TBST) and 5% skim milk, followed by incubation overnight at 4°C with primary antibodies diluted in Can Get Signal Solution 1 (TOYOBO). The primary antibodies used were anti-APOBEC3C antibody, anti-HSP60 antibody, and anti-GAPDH antibody (clone EPR16891, Abcam, Cambridge, UK). The membranes were then washed once with TBST and incubated for

1 hour at room temperature with horse radish peroxidase (HRP) -conjugated goat anti-rabbit antibody (Cell Signaling), diluted in Can Get Signal Solution 2 (TOYOBO). After further washing with TBST, the membranes were treated with Immobilon Western Chemiluminescent HRP substrate (Millipore), and luminescence was detected using Image Quant™ LAS 4000 (GE Healthcare, Chicago, IL).

Construction of gene expression vector

The APOBEC3H gene was amplified using the APOBEC3H gene primer set (F, 5'-GGAGAGCTGCCAAAAGTGAAACTT-3'; R, 5'-ACTTGGATGGGGCCAGGT-3') and KOD plus-neo with cDNA derived from AGS cells as a template. The amplified APOBEC3H gene product was inserted into the gene expression vector by modified circular polymerase extension cloning (CPER) (Quan J et al., *PLoS One*, 2009). The APOBEC3H gene was amplified again using the APOBEC3H-CPER primer set (F, 5'-ACAAAGATGATGACGATAAAGCTCT GTTAACAGCCGAAACA-3', R, 5'-GGCCCCCCCTCGAGTCAGGACTGCTTTATCCTCTC AAGCC-3') and KOD plus-neo with the PCR product derived from the APOBEC3H gene as a template. At the same time, the vector pCMV3Tag1A (Agilent, Santa Clara, CA) was amplified using the pCMV3Tag1A-CPER primer set (F, 5'-TTTATCGTCATCATCTTTGTAGTCCTTGT C-3', R, 5'-TGACTCGAGGGGGGGCC-3') and KOD plus-neo with the pCMV3Tag1A vector as

a template. The two PCR products were fused by CPER using KOD plus-neo (1 cycle of 94°C for 2 min; 15 cycles of 98°C for 10 sec, 55°C for 30 sec, 68°C for 3 min s; 1 cycle of 68°C for 10 min). The CPER product was transformed into *E. coli*, amplified, extracted, purified, and Sanger sequenced to confirm that the APOBEC3H gene was correctly amplified. The other APOBEC3 expression vectors and eGFP expression vector were gifted and used as previously prepared (Wang Z et al., *J Virol*, 2014). The plasmid, in which the FLAG sequence was inserted into the N-terminal of LMP2A and incorporated into the pcDNA3 vector (Hino R et al., *Cancer Res*, 2008), was created and provided by Dr. Teru Kanda of Tohoku Medical and Pharmaceutical University. All expression vectors were introduced into cells using Lipofectamine 2000 (Thermo Fisher Scientific).

Establishment of APOBEC 3C gene deleted AGS cell clones

APOBEC3C deleted AGS cell clones were created using the Clustered Regularly Interspaced Short Palindromic Repeats (CRISPR)-Cas9 system (Fu Y et al., *Nat Biotechnol*, 2014). Guide RNA for exon 3 of the APOBEC3C gene was designed using Benchling's guide RNA tool (https://benchling.com/crispr). Next, CRISPR RNA (crRNA) corresponding to the gene binding portion of the guide RNA and tracer RNA (trRNA) (IDT) were mixed in nuclease free duplex buffer, heated at 95°C for 5 minutes, and cooled at room temperature to form a crRNA-trRNA

complex. The RNA-Cas9 complex was formed by mixing the crRNA-trRNA complex and Cas9 protein (IDT) in Opti-MEM (Thermo Fisher Scientific) and incubating at room temperature for 5 minutes.

We seeded AGS cells at a density of 4×10^5 cells per well in a 6-well plate and incubated them overnight in a CO_2 incubator at 37°C. The following day, we prepared the RNA-Cas9 complex by mixing it with Lipofectamine 2000 in Opti-MEM and allowing the mixture to sit at room temperature for 20 minutes to form transfection complexes. These complexes were then added to the cells in each well, along with 1 mL of antibiotic-free medium. The cells were cultured at 37°C for 48 hours. After the incubation, we trypsinized the cells and diluted them to a concentration of 0.3 cells per 50 μL. Each well of a 96-well plate was then seeded with 50 μL of this cell suspension and incubated in a CO_2 incubator for 10 days to allow for clonal expansion. The resulting cell clones were analyzed by immunoblotting to confirm the absence of APOBEC3C expression. Additionally, the APOBEC3C gene sequence was determined to verify the successful introduction of the intended mutation.

Statistical analysis

Data are presented as the mean ± standard deviation from three independent experiments. Means of each data were analyzed by two-way unpaired t-test or one-way analysis of variance,

and P values less than 0.05 were considered statistically significant. All data were analyzed using GraphPad Prism 6 (GraphPad Software Inc., La Jolla, CA).

Results

1. Gastric epithelial cells persistently infected with EBV exhibited increased expression of APOBEC3 family members and increased C-to-T mutations in mtDNA

In AGS and MKN28 cells, the expression of APOBEC3A, APOBEC3B, APOBEC3C, and APOBEC3F genes was increased in cells persistently infected with eGFP-EBV compared to uninfected cells (**Figure 1A**). In contrast, APOBEC3G expression was lower in cells persistently infected with eGFP-EBV (**Figure 1A**). It has been reported that a C-to-T mutation can be confirmed in the D-loop gene of mtDNA, which is thought to be evidence of the action of APOBEC3 (Wakae K et al., *Sci Rep*, 2018). Therefore, we investigated whether C-to-T mutations are increased in the D-loop region of mtDNA in cells persistently infected with EBV using 3D-PCR; PCR amplification occurred at a lower annealing temperature in cells persistently infected with eGFP-EBV than in uninfected cells (**Figure 1B**). The mtDNA amplified at the lowest dissociation temperature in AGS cells infected with eGFP-EBV (**Figure 1B, black underline**) was extracted, purified, and sequenced. A 345-bp DNA sequence was obtained for seven clones, and the number of C-to-T or G-to-A mutations was counted (**Figure 1B, left**). Analysis of 2,415 bases from the gene sequences of the seven clones revealed 4 C-to-T mutations and 66 G-to-A mutations (**Figure 1B, right**). This corresponds to a gene mutation frequency of 2.9%. In addition, the average staining intensity of the expression region with respect to the mitochondria-specific

HSP60 protein was reduced by 17% in persistently EBV-infected cells compared to uninfected cells, with statistical significance (**Figure 1D**). Similarly, using immunoblotting, HSP60 protein expression was decreased in persistently EBV-infected cells compared to uninfected cells (**Figure 1E**). mtDNA copy number was also decreased by 35% in persistently EBV-infected cells compared to uninfected cells (**Figure 1F**). In conclusion, persistent EBV infection of gastric epithelial cells induces the expression of APOBEC3 family genes and increases C-to-T mutations in mtDNA, resulting in impaired mitochondrial replication.

2. Introduction of APOBEC3C gene into gastric epithelial cells increased C-to-T mutations in mtDNA

To determine which DNA editing enzyme causes the introduction of C-to-T mutations in mtDNA, the respective APOBEC3 family gene expression vectors was introduced into AGS cells and 3D-PCR was performed using mtDNA from the D-loop region. Compared to the introduction of empty vectors, trans-expression of APOBEC3A, APOBEC3B, APOBEC3C, and APOBEC3D resulted in increased C-to-T mutations in the mtDNA D-loop. Among them, transduced expression of APOBEC3C most strongly induced mutations (**Figure 2A**). DNA amplified at the lowest dissociation temperature in Fig. 2A (**Figure 2A black underline**) was extracted, purified and sequenced. The 345 bp long of each DNA sequence was determined for 11 clones and the

number of C to T or G to A mutations was counted (**Figure 2B top**). A total of 3,795 bases of the gene sequence for the 11 clones was sequenced, and one C-to-T mutation and 319 G-to-A mutations were introduced (**Figure 2B, bottom left**). The frequency of gene mutations was 8.4%. The motifs of the mutation-introduced sequences were biased toward GpC and CpC compared to the predicted values (**Figure 2B bottom right**). Overexpression of APOBEC3C, which frequently induced the C to T or G to A mutations in Figure 2B, also reduced mtDNA copy number (**Figure 2C**). Furthermore, the greater the amount of APOBEC3C expression vector introduced, the greater the C-to-T mutation in the mtDNA D-loop (**Figure 2D**).

These results indicate that among the APOBEC3 family genes, APOBEC3C is the most efficient gene for introducing C-to-T mutations into mtDNA.

3. APOBEC3C localizes to mitochondria in gastric epithelial cells

APOBEC3C has been reported to localize to the cytoplasm and nucleus in HeLa cells (Lackey L et al., *Cell Cycle*, 2013). Based on this report, we expressed APOBEC3C-GFP fusion protein in gastric epithelial AGS cells. The results showed that the control GFP was expressed both in the cytoplasm and nuclei, with substantial amounts observed in the nuclei and overlapped with the mitochondrial protein HSP60 at a small percentage of 10.9% (**Figure 3A**). On the other hand, the APOBEC3C-GFP fusion protein was strongly expressed in the cytoplasm and localized with

HSP60, overlapping with 53.8% (**Figure 3A**). Next, endogenously expressed APOBEC3C was immunostained and compared to mitochondria stained with antibodies against TFAM. As shown in **Figure 3B** left, using the intensity-based co-localization analysis (Furuyama W et al. *Microbiol Spectr,* 2024), we calculated the average brightness of TFAM staining from c to d, and the average brightness of APOBEC3C staining from a to b, and expressed the ratio of each (**Figure 3B right**). As a result, the co-localization of APOBEC3C and mitochondria increased from 27.1% in EBV-uninfected cells to 42.9% in EBV-infected cells (**Figure 3b right**). APOBEC3C was localized to the cytoplasm and mitochondria in EBV-uninfected cells, while APOBEC3C was localized to mitochondria with its increased expression in EBV-infected cells.

4. APOBEC3C, which is expressed during persistent EBV infection, causes mitochondrial damage

To clarify that the mtDNA mutations observed in persistently EBV-infected cells are caused by APOBEC3C, we generated APOBEC3C-deficient (APOBEC3C-KO) AGS cells clones 1 and 2 using the CRISPR-Cas9 method (**Figure 4A)**. Mutations were introduced into the APOBEC3C gene (**Figure 4A left**) and the expression of APOBEC3C protein was reduced (**Figure 4A right**). We have established eGFP-EBV(+) AGS cells and eGFP-EBV(+)APOBEC3C-KO AGS cells, by persistently infecting with eGFP-EBV. Mitochondrial HSP60 expression was weaker in eGFP-

EBV(+) AGS cells than in EBV(-) AGS cells, whereas there was no significant difference in HSP60 expression between eGFP-EBV(+)APOBEC3C-KO AGS cells and EBV(-)APOBEC3C-KO AGS cells (**Figure 4B upper, Figure 4B lower left**). Furthermore, the mtDNA copy number calculated based on the results of RT-PCR was less than 50% of that of EBV(-) AGS cells in eGFP-EBV(+) AGS cells, while the mtDNA copy number was higher in eGFP-EBV(+)APOBEC3C-KO AGS cells than in EBV(-)APOBEC3C-KO AGS cells (**Figure 4C**).

The results of the APOBEC3C knockout experiments suggest that the APOBEC3C gene is responsible for the damage and reduced number of mitochondrial genes observed in gastric epithelial cells persistently infected with EBV.

5. An EBV latent gene LMP2A causes mtDNA damage

In gastric epithelial cells that are persistently infected with EBV, EBV shows a type I latent infection and expresses a limited number of viral genes, including EBNA1, LMP2A, EBERs, and BART (Iizasa H et al. *Viruses*, 2012). Among these genes expressed in type I latent infection, we overexpressed LMP2A and confirmed that the introduction of mutations into the mtDNA gene in the D-loop region by the 3D-PCR method. The results showed accumulation of C-to-T mutations in the mtDNA genes in the D-loop region, since gene amplification was possible even at low annealing temperatures in response to the introduced amount of the LMP2A DNA (**Figure 5A**).

Compared to AGS cells persistently infected with wild-type EBV, APOBEC3C expression was reduced in AGS cells persistently infected with LMP2A-deficient EBV (**Figure 5B**). Subsequently, we conducted an experiment to reintroduce the LMP2A gene into AGS cells persistently infected with LMP2A-deficient EBV (**Supplemental Figure 1**). As a result, APOBEC3C expression increased in response to the amount of LMP2A DNA introduced (**Figure 5C**). These findings indicate that in gastric epithelial cells persistently infected with EBV, LMP2A promotes the expression of APOBEC3C, leading to mtDNA damage.

Discussion

Previous studies, including those on herpes simplex virus-1 (HSV-1), have demonstrated that release of mtDNA plays a key role in triggering innate immune pathways, such as the cGAS-STING axis, to combat viral infections (West AP et al., *Nature*, 2015). Interestingly, cells deficient in mitochondria exhibited reduced interferon expression during HSV-1 infection, highlighting the importance of mitochondrial integrity in antiviral immunity. Inspired by these findings, we hypothesized that EBV, which establishes persistent infection, might also employ mechanisms to disrupt mitochondrial function. In this study, we report that persistent EBV infection in gastric epithelial cells induces C-to-T mutations in mtDNA and reduces mtDNA copy number. These changes may aid the survival of persistently virus-infected cells by impairing

mitochondrial function and altering glucose metabolism. As a potential molecular mechanism, we demonstrated that the latent EBV gene LMP2A induces the expression of APOBEC3C, a DNA-editing enzyme. Suspène and colleagues reported that members of the APOBEC3 family, APOBEC3A and APOBEC3G, cause C-to-T mutations in the mtDNA of HeLa cells derived from cervical cancer (Suspène R et al., *Proc Natl Acad Sci U S A*, 2005). Wakae and colleagues reported that the latent EBV gene LMP1 induces the expression of APOBEC3B and APOBEC3F in nasopharyngeal carcinoma cells, and that forced expression of APOBEC3B and APOBEC3F in EBV-negative nasopharyngeal carcinoma cells leads to mtDNA mutations (Wakae K et al. *Cancer Med*, 2020). Our study revealed that the expression of APOBEC3A, APOBEC3B, and APOBEC3C in gastric epithelial cells induces genetic mutations in the mtDNA D-loop and reduces the amount of mtDNA. We found that APOBEC3C causes the most significant mitochondrial damage (**Figures 2A** and **4B**). In particular, we demonstrated that LMP2A expressed in gastric epithelial cells latently infected with EBV induces APOBEC3C, as shown using an LMP2A-deficient viruses (**Figure 5**). The data in Figures 1F and 2C indicate that EBV-infected cells exhibit lower mtDNA copy numbers than APOBEC3-overexpressing cells, despite harboring fewer mtDNA mutations. We hypothesize that part of the mutant DNA may have been removed in AGS-EBV cells. This could be attributed to the persistent expression of viral LMP2A

in AGS-EBV cells, which upregulates genes involved in DNA and RNA metabolism (Portis T et al. *Blood,* 2003).

Interestingly, APOBEC3C localized to mitochondria of gastric epithelial cells despite the absence of mitochondrial migration signals (**Figure 3**). In contrast, APOBEC3A and APOBEC3B are APOBEC3 family proteins that localize to the nucleus. This suggests that APOBEC3 family proteins capable of localizing to mitochondria may be more prone to inducing D-loop mutations. It is also possible that the intracellular localization of APOBEC3C varies depending on cell origin and differentiation. The mtDNA D-loop is a non-coding region rich in A and T nucleotide sequences, containing many target motifs for APOBEC3 (Swanton C et al., *Cancer Discov*, 2015). Although mutations in the D-loop sequence have been observed in various tumors, their physiological significance remains unclear (Cavalcante GC et al., *BMC Genom Data*, 2022, Nicholls TJ & Minczuk M. *Exp Gerontol*, 2014). However, in mitochondria of all organisms, the D-loop serves as the initiation site for mtDNA replication, and mitochondrial RNA transcription also begins at the D-loop (Nicholls TJ & Minczuk M. *Exp Gerontol*, 2014). Therefore, the D-loop is considered an essential region for mitochondrial replication. Consequently, the accumulation of C-to-T mutations in the D-loop may impair mitochondrial replication.

We have shown that persistent infection of gastric epithelial cells with EBV induces APOBEC3C expression, targeting and impairing the mitochondrial D-loop, leading to a reduction

in the amount of mtDNA. Mussil B et al. demonstrated that cytoplasmic mtDNA, released due to cellular stress or genotoxic agents, can become a target for APOBEC3-mediated cytidine deamination in EBV-infected cells. Their findings underline the dynamic interaction between mtDNA stress and APOBEC3 activity (Mussil B et al. *Sci Rep,* 2019). It has also been reported that the latent EBV genes LMP1 or LMP2A inhibit mitochondrial function (Pal AD et al., *Carcinogenesis*, 2014). These findings suggest that EBV creates a cellular environment favorable for maintaining viral infection by inducing APOBEC3C expression in gastric epithelial cells. The decrease in mitochondrial number reduces the efficiency of oxidative phosphorylation and increases ATP production via glycolysis, leading to the Warburg effect.

While our study identifies potential changes in mtDNA levels under the studied conditions, we did not directly assess the functional consequences of these changes, such as their effects on mitochondrial bioenergetics or cellular metabolism. However, previous studies have shown that mtDNA mutations can impair oxidative phosphorylation, potentially triggering compensatory metabolic shifts such as increased glycolysis (Wallace DC, *Nat Rev Cancer*, 2012). Similarly, cytoplasmic mtDNA targeted by APOBEC3 proteins has been linked to cellular stress responses (Mussil B et al. *Sci Rep,* 2019). Consequently, persistently EBV-infected cells may become resistant to apoptosis, leading to tumorigenic transformation in the long term.

Funding

This research was supported by Otsuka Toshimi Scholarship Foundation, SGH Foundation, Hashiya Foundation, the Honjo Foundation, JSPS KEKNHI (18K15168, 22K07101, 24K11632), and Kobayashi Foundation. The authors also thank the technological expertise of the Interdisciplinary Center for Science Research, Organization for Research and Academic Information, Shimane University.

Acknowledgments

The authors show sincere gratitude to Yuichi Kanehiro, Emi Kurauchi and Noriko Itoh for their assistance with the office work and experiments.

Conflict of interest

The authors declare no conflicts of interests.

Information of authors

Aung Phyo Wai <aungpwai@med.shimane-u.ac.jp>

Department of Microbiology, Faculty of Medicine, Shimane University, 89-1 Enya, Izumo, Shimane, Japan

Richardo Timmy <timmy.richardo@uni-tuebingen.de>

Department of Immunology, Innate Immunity Research Group, University of Tübingen, Tübingen, Germany

Kousho Wakae <wakae@niid.go.jp>

Department of Virology II, National Institute of Infectious Disease, Tokyo, Japan

ORCID: https://orcid.org/0000-0001-7767-6795

Shunpei Okada <s.okada@med.shimane-u.ac.jp>

Department of Microbiology, Faculty of Medicine, Shimane University, 89-1 Enya, Izumo, Shimane, Japan

Masamichi Muramatsu <muramatsu@fbri.org>

Department of Infectious Disease Research, Foundation for Biomedical Research and Innovation at Kobe, Kobe, Hyogo, Japan

Hironori Yoshiyama <yosiyama@med.shimane-u.ac.jp>

Department of Microbiology, Faculty of Medicine, Shimane University, 89-1 Enya, Izumo, Shimane, Japan

ORCID: https://orcid.org/0000-0001-7588-278X

Hisashi Iizasa <iizasah@med.shimane-u.ac.jp>

Department of Microbiology, Faculty of Medicine, Shimane University, 89-1 Enya, Izumo, Shimane, Japan

ORCID: https://orcid.org/0000-0002-9202-2666

References

1. Burke AP, Yen TS, Shekitka KM, Sobin LH. Lymphoepithelial carcinoma of the stomach with Epstein-Barr virus demonstrated by polymerase chain reaction. *Mod Pathol* 3(3):377-380 (1990).

2. Imai S, Koizumi S, Sugiura M, Tokunaga M, Uemura Y, Yamamoto N, Tanaka S, Sato E, Osato T. Gastric carcinoma: monoclonal epithelial malignant cells expressing Epstein-Barr virus latent infection protein. *Proc Natl Acad Sci U S A* 91(19):9131-9135 (1994).

3. Henle W, Henle G, Zajac BA, Pearson G, Waubke R, Scriba M. Differential reactivity of human serums with early antigens induced by Epstein-Barr virus. *Science* 169(3941):188-190 (1970).

4. Iizasa H, Nanbo A, Nishikawa J, Jinushi M, Yoshiyama H. Epstein-Barr Virus (EBV)-associated gastric carcinoma. *Viruses* 4(12):3420-3439 (2012).

5. Cancer Genome Atlas Research Network. Comprehensive molecular characterization of gastric adenocarcinoma. *Nature* 513(7517):202-209 (2014).

6. Swanton C, McGranahan N, Starrett GJ, Harris RS. APOBEC Enzymes: Mutagenic Fuel for Cancer Evolution and Heterogeneity. *Cancer Discov* 5(7):704-712 (2015).

7. Harris RS, Bishop KN, Sheehy AM, Craig HM, Petersen-Mahrt SK, Watt IN, Neuberger MS, Malim MH. DNA deamination mediates innate immunity to retroviral infection. *Cell* 113 (6): 803-809 (2003).

8. Suspène R, Guétard D, Henry M, Sommer P, Wain-Hobson S, Vartanian JP. Extensive editing of both hepatitis B virus DNA strands by APOBEC3 cytidine deaminases in vitro and in vivo. *Proc Natl Acad*

Sci U S A 102(23):8321-8326 (2005).

9. Vartanian JP, Guétard D, Henry M, Wain-Hobson S. Evidence for editing of human papillomavirus DNA by APOBEC3 in benign and precancerous lesions. *Science* 320(5873):230-233 (2008).

10. Wang Z, Wakae K, Kitamura K, Aoyama S, Liu G, Koura M, Monjurul AM, Kukimoto I, Muramatsu M. APOBEC3 deaminases induce hypermutation in human papillomavirus 16 DNA upon beta interferon stimulation. *J Virol* 88(2):1308-1317 (2014).

11. Cheng AZ, Yockteng-Melgar J, Jarvis MC, Malik-Soni N, Borozan I, Carpenter MA, McCann JL, Ebrahimi D, Shaban NM, Marcon E, Greenblatt J, Brown WL, Frappier L, Harris RS. Epstein-Barr virus BORF2 inhibits cellular APOBEC3B to preserve viral genome integrity. *Nat Microbiol* 4(1):78-88 (2019)

12. Burns MB, Lackey L, Carpenter MA, Rathore A, Land AM, Leonard B, Refsland EW, Kotandeniya D, Tretyakova N, Nikas JB, Yee D, Temiz NA, Donohue DE, McDougle RM, Brown WL, Law EK, Harris RS. APOBEC3B is an enzymatic source of mutation in breast cancer. *Nature* 494(7437):366-370 (2013).

13. Refsland EW, Stenglein MD, Shindo K, Albin JS, Brown WL, Harris RS. Quantitative profiling of the full APOBEC3 mRNA repertoire in lymphocytes and tissues: implications for HIV-1 restriction. *Nucleic Acids Res* 38(13):4274-4284 (2010).

14. Coursey TL, McBride AA. Hitchhiking of Viral Genomes on Cellular Chromosomes. *Annu Rev Virol*

6(1):275-296 (2019).

15. Kanda T, Horikoshi N, Murata T, Kawashima D, Sugimoto A, Narita Y, Kurumizaka H, Tsurumi T. Interaction between basic residues of Epstein-Barr virus EBNA1 protein and cellular chromatin mediates viral plasmid maintenance. *J Biol Chem* 288(33):24189-99 (2013).

16. Pal AD, Basak NP, Banerjee AS, Banerjee S. Epstein-Barr virus latent membrane protein-2A alters mitochondrial dynamics promoting cellular migration mediated by Notch signaling pathway. *Carcinogenesis* 35(7):1592-1601 (2014).

17. Wang Z, Lv Z, Xu Q, Sun L, Yuan Y. Identification of differential proteomics in Epstein-Barr virus-associated gastric cancer and related functional analysis. *Cancer Cell Int* 21(1):368 (2021).

18. Shidara Y, Yamagata K, Kanamori T, Nakano K, Kwong JQ, Manfredi G, Oda H, Ohta S. Positive contribution of pathogenic mutations in the mitochondrial genome to the promotion of cancer by prevention from apoptosis. *Cancer Res* 65(5):1655-1663 (2005).

19. Wallace DC. Mitochondria and cancer. *Nat Rev Cancer* 12(10):685-698 (2012).

20. Nakatani H, Tahara E, Yoshida T, Sakamoto H, Suzuki T, Watanabe H, Sekiguchi M, Kaneko Y, Sakurai M, Terada M, Sugimura T. Detection of amplified DNA sequences in gastric cancers by a DNA renaturation method in gel. *Jpn J Cancer Res* 77:849-853 (1986).

21. Maruo S, Yang L, Takada K. Roles of Epstein-Barr virus glycoproteins gp350 and gp25 in the infection of human epithelial cells. *J Gen Virol* 82(Pt 10):2373-2383 (2001).

22. Konishi K, Maruo S, Kato H, Takada K. Role of Epstein-Barr virus-encoded latent membrane protein 2A on virus-induced immortalization and virus activation. *J Gen Virol* 82(Pt 6):1451-1456 (2001).

23. Kitamura K, Wang Z, Chowdhury S, Simadu M, Koura M, Muramatsu M. Uracil DNA glycosylase counteracts APOBEC3G-induced hypermutation of hepatitis B viral genomes: excision repair of covalently closed circular DNA. *PLoS Pathog* 9(5):e1003361 (2013).

24. Furuyama W, Yamada K, Sakaguchi M, Marzi A, Nanbo A. Marburg virus exploits the Rab11-mediated endocytic pathway in viral-particle production. *Microbiol Spectr* 12(9):e0026924 (2024).

25. Venegas V, Wang J, Dimmock D, Wong LJ. Real-time quantitative PCR analysis of mitochondrial DNA content. *Curr Protoc Hum Genet* Chapter 19:Unit 19.7. (2011)

26. Quan J, Tian J. Circular polymerase extension cloning of complex gene libraries and pathways. *PLoS One* 4(7):e6441 (2009).

27. Hino R, Uozaki H, Inoue Y, Shintani Y, Ushiku T, Sakatani T, Takada K, Fukayama M. Survival advantage of EBV-associated gastric carcinoma: survivin up-regulation by viral latent membrane protein 2A. *Cancer Res* 68(5):1427-35 (2008).

28. Fu Y, Sander JD, Reyon D, Cascio VM, Joung JK. Improving CRISPR-Cas nuclease specificity using truncated guide RNAs. *Nat Biotechnol* 32(3):279-284 (2014).

29. Wakae K, Nishiyama T, Kondo S, Izuka T, Que L, Chen C, Kase K, Kitamura K, Mohiuddin M, Wang Z, Ahasan MM, Nakamura M, Fujiwara H, Yoshizaki T, Hosomochi K, Tajima A, Nakahara T, Kiyono

T, Muramatsu M. Keratinocyte differentiation induces APOBEC3A, 3B, and mitochondrial DNA hypermutation. *Sci Rep* 8(1):9745 (2018).

30. Lackey L, Law EK, Brown WL, Harris RS. Subcellular localization of the APOBEC3 proteins during mitosis and implications for genomic DNA deamination. *Cell Cycle* 12(5):762-772 (2013).

31. West AP, Khoury-Hanold W, Staron M, Tal MC, Pineda CM, Lang SM, Bestwick M, Duguay BA, Raimundo N, MacDuff DA, Kaech SM, Smiley JR, Means RE, Iwasaki A, Shadel GS. Mitochondrial DNA stress primes the antiviral innate immune response. *Nature* 520(7548):553-557 (2015).

32. Wakae K, Kondo S, Pham HT, Wakisaka N, Que L, Li Y, Zheng X, Fukano K, Kitamura K, Watashi K, Aizaki H, Ueno T, Moriyama-Kita M, Ishikawa K, Nakanishi Y, Endo K, Muramatsu M, Yoshizaki T. EBV-LMP1 induces APOBEC3s and mitochondrial DNA hypermutation in nasopharyngeal cancer. *Cancer Med* 9(20):7663-7671 (2020).

33. Portis T, Dyck P, Longnecker R. Epstein-Barr virus (EBV) LMP2A induces alterations in gene transcription similar to those observed in Reed-Sternberg cells of Hodgkin lymphoma. *Blood* 102(12):4166–4178 (2003).

34. Cavalcante GC, Ribeiro-Dos-Santos Â, de Araújo GS. Mitochondria in tumour progression: a network of mtDNA variants in different types of cancer. *BMC Genom Data* 23(1):16 (2022).

35. Nicholls TJ, Minczuk M. In D-loop: 40 years of mitochondrial 7S DNA. *Exp Gerontol* 56:175-181 (2014).

36. Mussil B, Suspène R, Caval V, Durandy A, Wain-Hobson S, Vartanian JP. Genotoxic stress increases cytoplasmic mitochondrial DNA editing by human APOBEC3 mutator enzymes at a single cell level. *Sci Rep* 9(1):3109 (2019)

Figure Legends

Figure 1. Persistent EBV Infection Induces APOBEC3 Family Gene Expression and Increases mtDNA Mutations

(A) Expression levels of APOBEC3 family mRNAs in AGS and MKN28 cells persistently infected with EBV. The expression levels are calculated relative to those of uninfected cells, set to 1. Open squares represent uninfected cells, and black squares represent EBV-infected cells.

(B) Detection of mutations in the mtDNA D-loop region of persistently EBV-infected cells using 3D-PCR.

(C) Gene mutations in the mtDNA D-loop region of EBV-infected cells. DNA from EBV(+)AGS cells was used to perform 3D-PCR on the D-loop region DNA. The DNA amplified at the lowest denaturation temperature (underlined in black) was cloned, and 7 clones were sequenced by the Sanger method. Blue vertical lines indicate C-to-T conversions, red vertical lines indicate G-to-A conversions, and black vertical lines indicate other mutations. There were 87 C-to-T and 65 G-to-A recognized motifs in the 345 bp DNA sequence of the D-loop region. The number of mutations in the motifs for each of the 7 clones is shown (left). The number of mutations in a total

of 2,415 bases across the 7 clone sequences is 66 C-to-T and 4 G-to-A, which are represented in the table (right).

(D) Measurement of mean HSP60 fluorescence intensity in EBV-infected and uninfected cells. Red indicates HSP60-positive cells, and nuclear DNA is counterstained with DAPI. The graph represents the mean fluorescence intensity of HSP60 in 20 randomly selected cells.

(E) Expression of HSP60 protein in EBV-infected and uninfected cells. HSP60 protein levels were detected by Western blotting in uninfected AGS cells and EBV-infected AGS cells, with GAPDH used as an internal control.

(F) mtDNA copy number in EBV-infected and uninfected cells. The mtDNA copy number was normalized to the copy number of the GAPDH gene. Open squares represent uninfected cells, and black squares represent EBV-infected cells. A: APOBEC3A, B: APOBEC3B, C: APOBEC3C, D: APOBEC3D, F: APOBEC3F, G: APOBEC3G, H: APOBEC3H, mtDNA: mitochondrial DNA.

Figure 2. APOBEC3C Induces C-to-T Mutations in mtDNA of Gastric Epithelial Cells

(A) Mutation induction in the mtDNA D-loop region by overexpression of individual APOBEC3 family genes. AGS cells were transfected with 2 μg of expression vectors for APOBEC3A, B, C, D, F, and H, respectively, and 3D-PCR was performed on the D-loop region DNA 48 hours after transfection.

(B) Gene mutations in the mtDNA D-loop region of APOBEC3C-overexpressing cells. DNA from AGS cells transfected with the APOBEC3C gene was used to perform 3D-PCR on the D-loop region DNA. The DNA amplified at the lowest denaturation temperature (underlined in black) was cloned, and 11 clones were sequenced by the Sanger method. Blue vertical lines indicate C-to-T conversions, red vertical lines indicate G-to-A conversions, and black vertical lines indicate other mutations. There were 87 C-to-T and 65 G-to-A recognized motifs in the 345 bp DNA sequence of the D-loop region. The number of mutations in the motifs for each of the 11 clones is shown (upper right). The number of mutations in a total of 3,795 bases across the 11 clone sequences is represented in the table (lower left). The 5'-dinucleotide context analysis results are shown as expected values (gray bars) and actual results after APOBEC3C gene introduction (black bars) (lower right).

(C) mtDNA copy number in APOBEC3C-overexpressing cells. The mtDNA copy number per cell in AGS cells transfected with the APOBEC3C gene was determined by qPCR using total DNA as the template. White bars represent mock, and black bars represent the APOBEC3C expression vector.

(D) Dose-dependent mtDNA D-loop region mutations induced by APOBEC3C. AGS cells were transfected with 10, 100, 1,000, or 2,000 ng of APOBEC3C expression vector, and 3D-PCR was performed on the DNA isolated 48 hours post-transfection. A3A: APOBEC3A, A3B:

APOBEC3B, A3C: APOBEC3C, A3D: APOBEC3D, A3F: APOBEC3F, A3G: APOBEC3G, A3H: APOBEC3H, mtDNA: mitochondrial DNA.

Figure 3. APOBEC3C Primarily Localizes to Mitochondria in Gastric Epithelial Cells

(A) In gastric epithelial cells, APOBEC3C predominantly localizes to mitochondria. AGS cells attached to poly-L-lysine-coated coverslips were transfected with GFP or APOBEC3C-GFP expression vectors. The cells were stained with a mitochondria-specific HSP60 antibody, followed by an Alexa Fluor 568-labeled goat anti-rabbit IgG antibody, and then observed under a confocal microscope (top). Green indicates GFP, and red indicates HSP60. In the merged image of GFP and HSP60 staining, fluorescence intensities along a white line section were plotted, with GFP intensity shown as a green line and HSP60 staining intensity as a red line (bottom left). The colocalization of APOBEC3C and HSP60 was assessed by measuring the mean fluorescence intensities of GFP and HSP60 staining in three cells, calculating their ratio, and expressing it as a percentage of colocalization (bottom right).

(B) Localization of endogenously expressed APOBEC3C and mitochondria-specific TFAM. The proteins were immunostained (TFAM: white, APOBEC3C: red) (left). To compare the localization of the proteins, the mean fluorescence intensity of TFAM from c to d and that of the

APOBEC3C antibody from a to b were measured. The ratios were calculated and expressed as the percentage of colocalization (right). A3C: APOBEC3C.

Figure 4. APOBEC3C Reduces mtDNA Copy Number in Persistently EBV-Infected Gastric Epithelial Cells

(A) Establishment of APOBEC3C-knockout cells using genome editing. Left: The gene map of the APOBEC3C gene consisting of four exons and the targeted sequences of the APOBEC3C-knockout mutant clones 1 and 2 generated by the CRISPR/Cas9 method. The underlined region indicates the guide RNA binding sequence (target sequence) in exon 3 of the APOBEC3C gene. A3C: APOBEC3C, PAM: Protospacer Adjacent Motif. Right: Western blotting results showing the expression of APOBEC3C in total lysates from wild-type cells and APOBEC3C-mutant clones 1 and 2, using an anti-APOBEC3C antibody. The top panel shows APOBEC3C expression, and the bottom panel shows GAPDH as a loading control.

(B) The reduction in HSP60 expression due to persistent EBV infection is not observed in APOBEC3C-knockout cells. AGS cells and APOBEC3C-knockout AGS clone 1 cells, both uninfected and persistently infected with recombinant EBV, were prepared. Mitochondria-specific HSP60 protein was immunostained and shown in red. Nuclear DNA was counterstained with DAPI. White bars represent EBV-negative cells, and gray bars represent persistently EBV-

infected cells. The average intensity of HSP60 staining was measured in 20 randomly selected cells and is displayed as a box-and-whisker plot using a confocal microscope.

(C) APOBEC3C-knockout cells do not show a decrease in mtDNA copy number due to persistent EBV infection. Total DNA was extracted from AGS cells and APOBEC3C-knockout AGS clone 1 cells, both uninfected and persistently infected with recombinant EBV, and the mtDNA copy number was calculated. mtDNA: mitochondrial DNA.

Figure 5. The EBV Latent Infection Gene LMP2A Induces mtDNA Damage

(A) mtDNA mutations in LMP2A-overexpressing cells. AGS cells were transfected with 100, 500, or 1000 ng of LMP2A expression vector. After 48 hours, total DNA was extracted for 3D-PCR analysis of the mitochondrial D-loop region.

(B) The expression level of APOBEC3C decreases in wild-type EBV-infected cells, but not in LMP2A-deficient EBV-infected AGS cells. Total RNA was extracted from uninfected AGS cells, EBV-infected AGS cells, and LMP2A-deficient EBV-infected AGS cells. RT-qPCR was performed, and the relative expression of the APOBEC3C gene was calculated with uninfected AGS cells set as 1. White bar: uninfected AGS cells; black bar: wild-type EBV-infected AGS cells; gray bar: LMP2A-deficient EBV-infected AGS cells. A3C: APOBEC3C.

(C) Introduction of LMP2A induces APOBEC3C expression. Various amounts of LMP2A expression vector (0, 1, 10, and 100 ng) were transfected into AGS cells persistently infected with LMP2A-deficient EBV. Total RNA was extracted after 48 hours and RT-qPCR was performed to calculate the relative expression of the APOBEC3C gene, with the expression in cells not transfected with LMP2A set as 1. White bar: control AGS cells; light gray bar: AGS cells transfected with 1 ng of LMP2A; dark gray bar: AGS cells transfected with 10 ng of LMP2A; black bar: AGS cells transfected with 100 ng of LMP2A. A3C: APOBEC3C.

Table 1. Primer sequences for PCR

Gene Namae	Forword primer (5'- -3')	Reverse primer (5'- -3')
APOBEC3A	ATGGCATTGGAAGGCATAAG	CAAAGAAGGAACCAGGTCCA
APOBEC3B	TTCGAGGCCAGGTGTATTTCA	CAGAGATGGTCAGGGTGACA
APOBEC3C	AAGGACGCTGTAAGCAGGAAG	CTTCATCGGGTTTCTGATCTGTG
APOBEC3D	ACCCAAACGTCAGTCGAATC	GCTCAGCCAAGAATTTGGTC
APOBEC3F	GAAACACAGTGGAGCGAATG	GAAATGGGGCTCTGATGAAAG
APOBEC3G	GGTCAGAGGACGGCATGAGA	GCAGGACCCAGGTGTCATTG
APOBEC3H	CCCGCCTGTACTACCACTGG	GGGTTGAAGGAAAGCGGTTT
GAPDH	AATCCCATCACCATCTTCCA	TGGACTCCACGACGTACTCA

Table 2. Primer sequences for 3D-PCR

Gene Name		Forward (5'-, -3')	Reverse (5'-, -3')
D-loop	1st	GGCAGAGATGTGTTTAAGTGCTG	ACCACCATCCTCCGTGAAAT
	2nd	TCTGTGTGGAAAGTGGCTGT	CTGGTTCCTACTTCAGGGTCA

Table 3. 3D-PCR condition

Gene Name	Pre-Denaturation	Denaturation	Annealing	Extension	Final Extension
		1st PCR			
D-loop	95°C 1 min	95°C 30 sec	56°C 30 sec	72°C 30 sec	72°C 1 min
		2nd PCR			
D-loop	84.4-81.5°C 1 min	84.4-81.5°C 15 sec	57°C 15 sec	72°C 5 sec	72°C 1 min

Supplementary Materials and Methods

Immunoblotting

Two million EBV-infected or-uninfected AGS cells were lysed using MEM-PER Plus Membrane Protein Extraction kit (ThermoFisher Scientific) containing protease inhibitor (cOmplete™ Mini Protease Inhibitor Cocktail, Sigma-Aldrich). Then, 1.8 μg of membrane fraction protein was electrophoresed using 7.5% SDS-PAGE and transferred to a 0.2 μm PVDF membrane (Millipore, Kenilworth, NJ). The PVDF membrane was treated with Block ACE to prevent nonspecific antibody binding. 15F9 (Abcam, Cambridge, UK) and EP1845Y (Abcam) were used to detect LMP2A and NA^+/K^+-ATPase, respectively. The membranes were washed three times with TBST and incubated for 45 min at room temperature with HRP-conjugated goat anti-rat antibody or anti-rabbit antibody (Cell Signaling). After further washing with TBST, the membranes were treated with Immobilon Western Chemiluminescent HRP substrate (Millipore), and luminescent signals were detected by X-ray film.

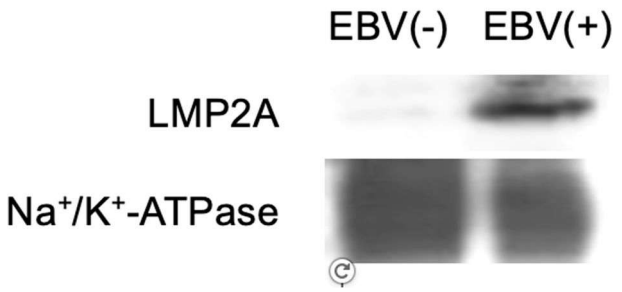

Supplementary Figure 1. EBV-infected epithelial AGS cell expresses LMP2A. LMP2A protein and Na^+/K^+-ATPase were detected using an immunoblotting method. Na^+/K^+-ATPase is used as an internal control for membrane-anchored protein. EBV(-): EBV-negative AGS cell, EBV(+): EBV-infected AGS cell.

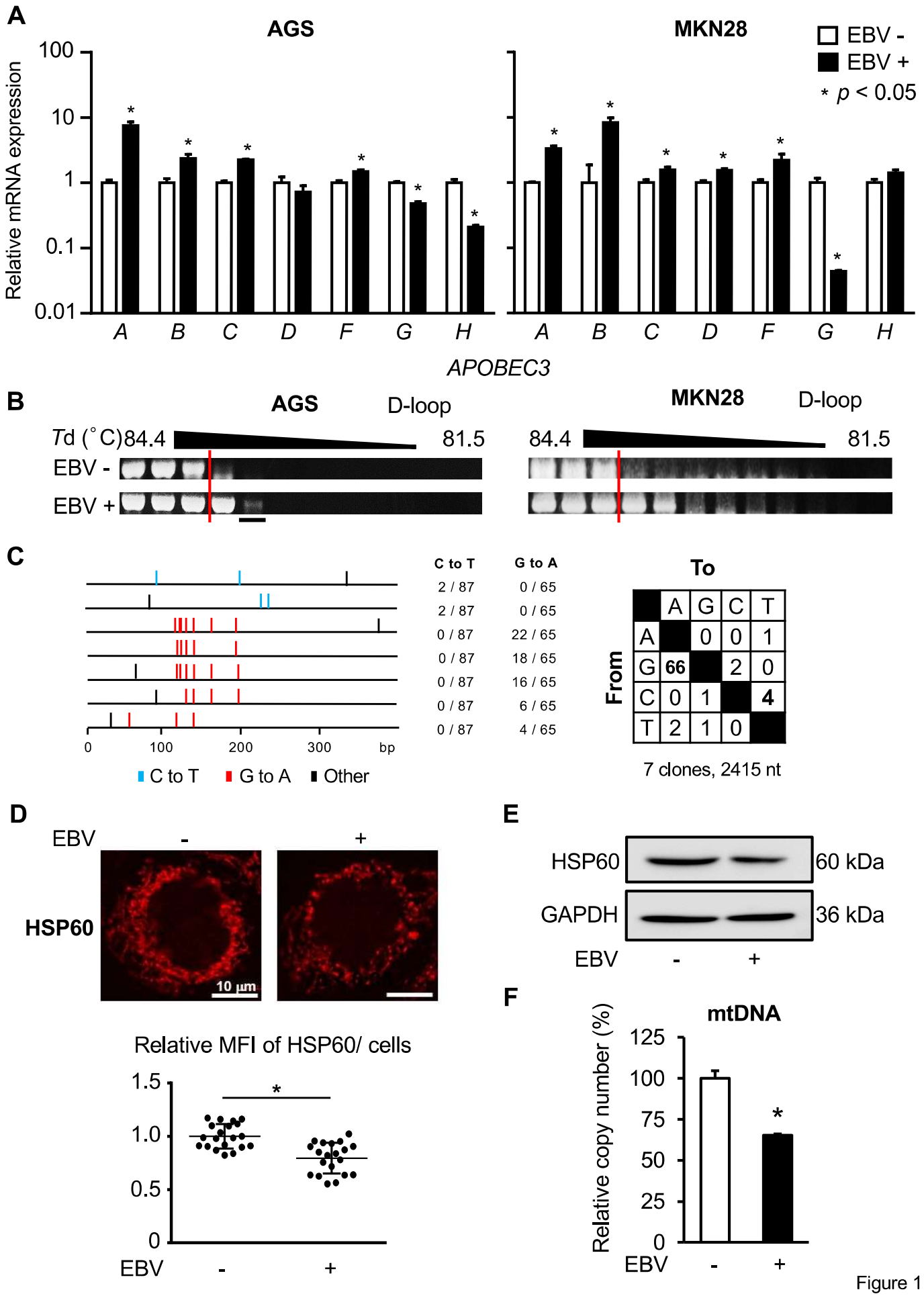
A
AGS
MKN28
EBV -
EBV +
* p < 0.05
Relative mRNA expression
100
10
1
0.1
0.01
A B C D F G H
APOBEC3
B
AGS
D-loop
MKN28
D-loop
Td (°C)84.4
81.5
EBV -
EBV +
C
C to T
G to A
2 / 87
0 / 65
2 / 87
0 / 65
0 / 87
22 / 65
0 / 87
18 / 65
0 / 87
16 / 65
0 / 87
6 / 65
0 / 87
4 / 65
0
100
200
300
bp
C to T
G to A
Other
To
From
A G C T
A 0 0 1
G 66 2 0
C 0 1 4
T 2 1 0
7 clones, 2415 nt
D
EBV
-
+
HSP60
10 μm
Relative MFI of HSP60/ cells
1.5
1.0
0.5
0
EBV
-
+
E
HSP60
60 kDa
GAPDH
36 kDa
EBV
-
+
F
mtDNA
Relative copy number (%)
125
100
75
50
25
0
EBV
-
+

Figure 1

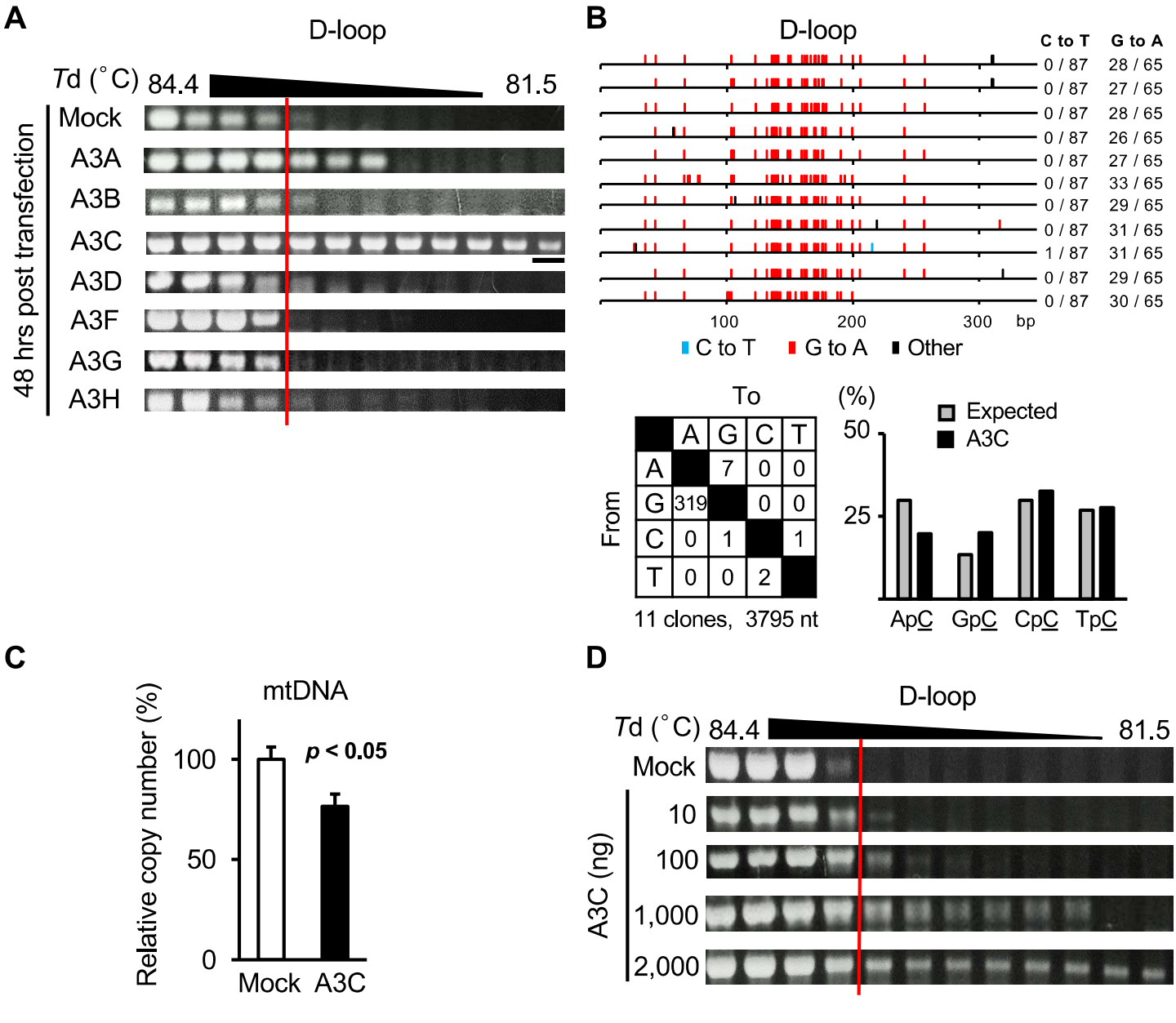
A
D-loop
Td (˚C) 84.4
81.5
48 hrs post transfection
Mock
A3A
A3B
A3C
A3D
A3F
A3G
A3H
B
D-loop
C to T
G to A
0 / 87 28 / 65
0 / 87 27 / 65
0 / 87 28 / 65
0 / 87 26 / 65
0 / 87 27 / 65
0 / 87 33 / 65
0 / 87 29 / 65
0 / 87 31 / 65
1 / 87 31 / 65
0 / 87 29 / 65
0 / 87 30 / 65
100
200
300
bp
C to T
G to A
Other
To
From
A G C T
A 7 0 0
G 319 0 0
C 0 1 1
T 0 0 2
11 clones, 3795 nt
(%)
50
25
Expected
A3C
ApC
GpC
CpC
TpC
C
mtDNA
Relative copy number (%)
100
50
0
p < 0.05
Mock
A3C
D
D-loop
Td (˚C) 84.4
81.5
Mock
A3C (ng)
10
100
1,000
2,000

Figure 2

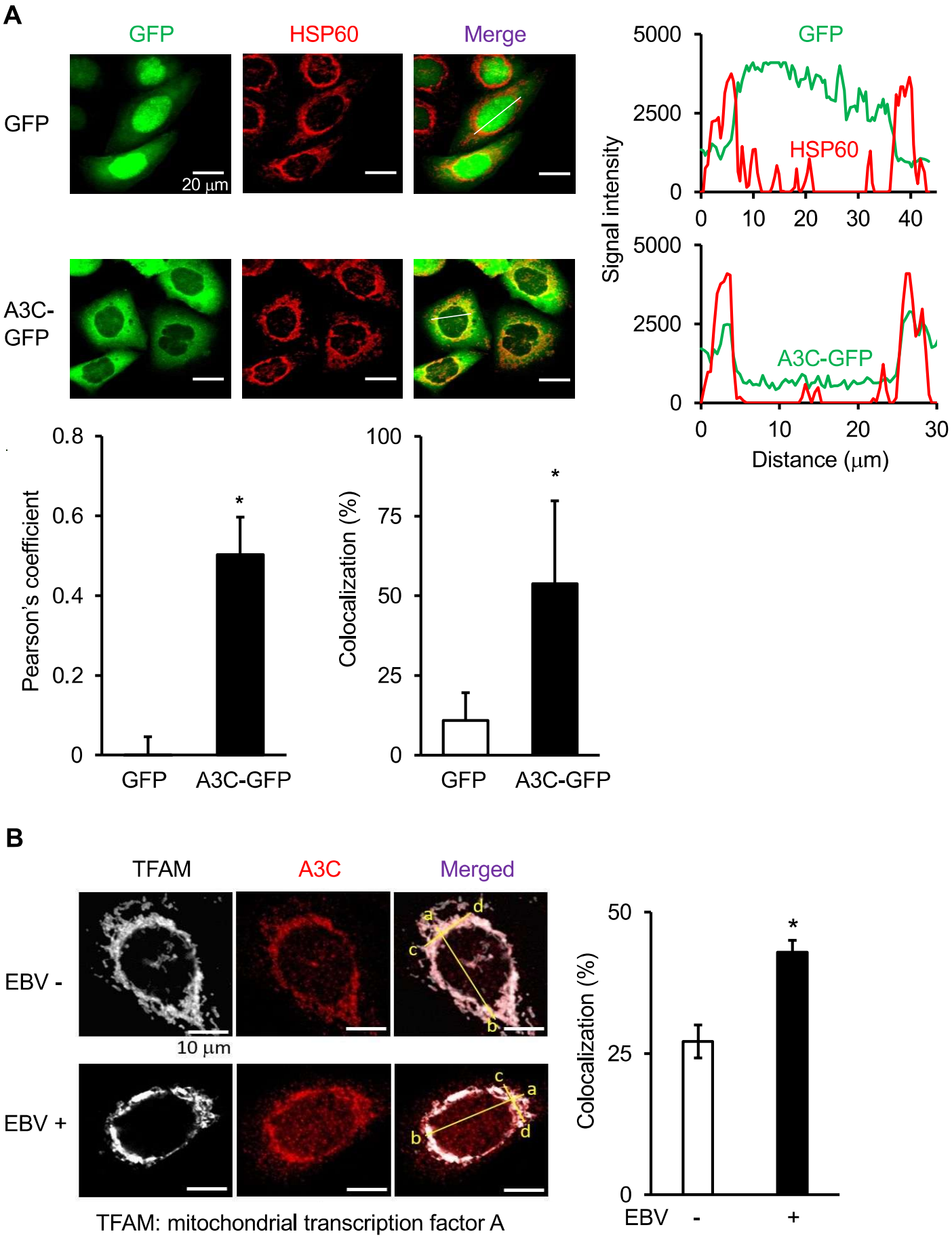
A
GFP
HSP60
Merge
GFP
20 μm
A3C-GFP
5000
2500
0
GFP
HSP60
Signal intensity
0 10 20 30 40
5000
2500
0
A3C-GFP
0 10 20 30
Distance (μm)
0.8
0.6
0.4
0.2
0
Pearson's coefficient
*
GFP
A3C-GFP
100
75
50
25
0
Colocalization (%)
*
GFP
A3C-GFP
B
TFAM
A3C
Merged
EBV -
a
d
c
b
10 μm
EBV +
c
a
b
d
50
25
0
Colocalization (%)
*
EBV
-
+
TFAM: mitochondrial transcription factor A

Figure 3

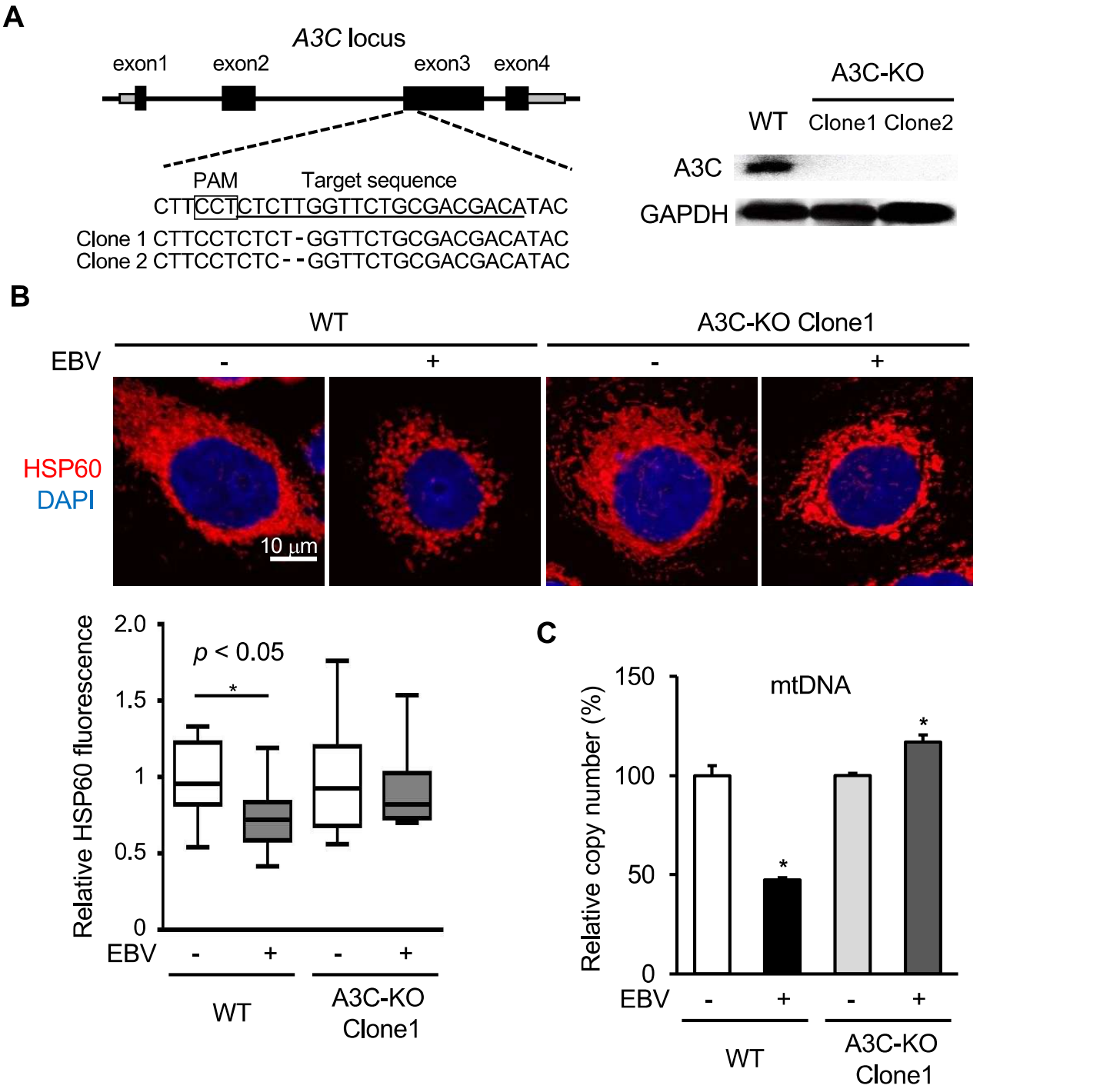
A
A3C locus
exon1
exon2
exon3
exon4
PAM
Target sequence
CTTCCTCTCTTGGTTCTGCGACGACATAC
Clone 1 CTTCCTCTCT-GGTTCTGCGACGACATAC
Clone 2 CTTCCTCTC--GGTTCTGCGACGACATAC
A3C-KO
WT
Clone1 Clone2
A3C
GAPDH
B
WT
A3C-KO Clone1
EBV
-
+
-
+
HSP60
DAPI
10 μm
Relative HSP60 fluorescence
2.0
1.5
1
0.5
0
p < 0.05
*
EBV
-
+
-
+
WT
A3C-KO
Clone1
C
mtDNA
Relative copy number (%)
150
100
50
0
*
*
EBV
-
+
-
+
WT
A3C-KO
Clone1

Figure 4

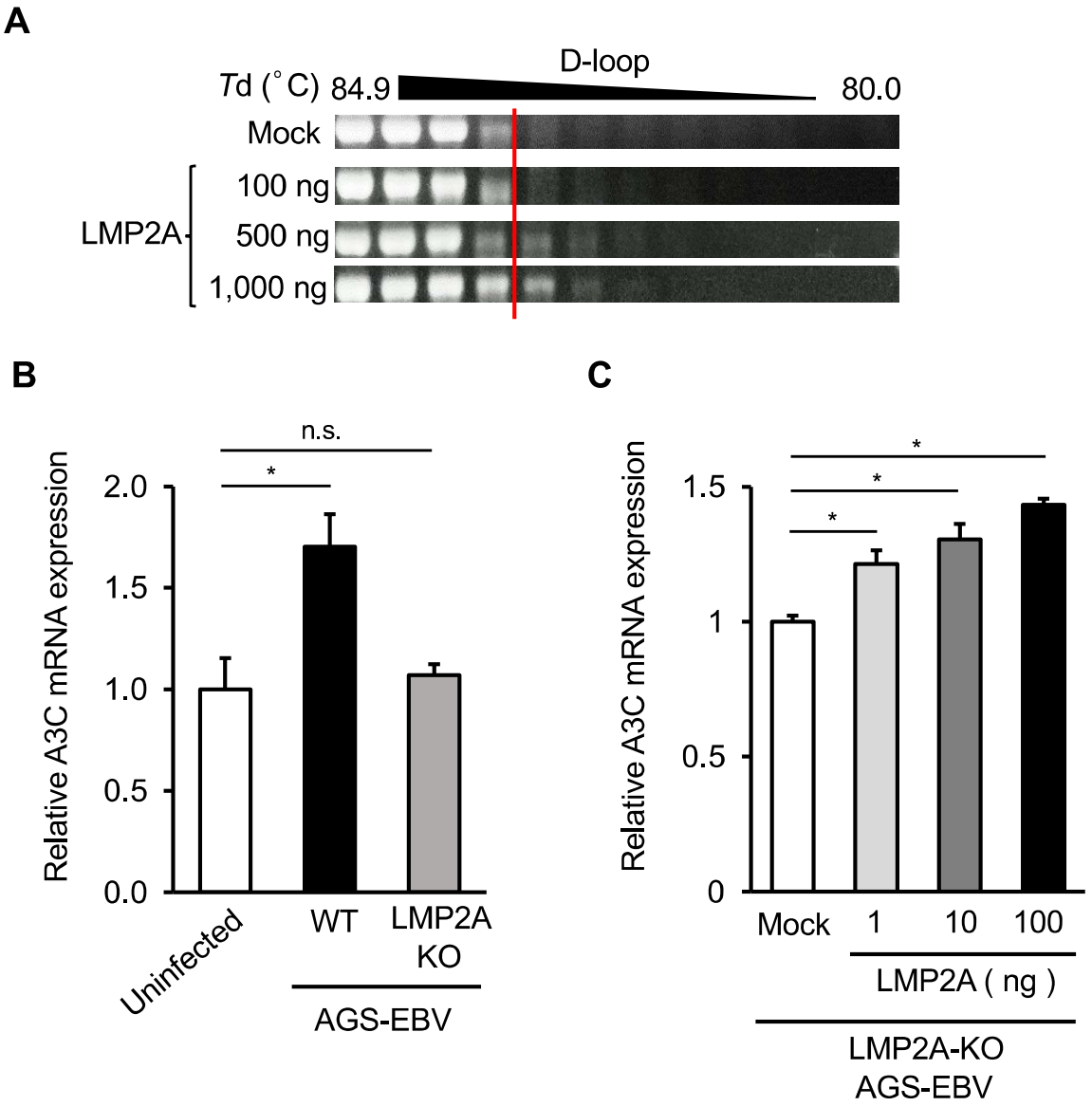
A
D-loop
Td (˚C) 84.9
80.0
Mock
LMP2A
100 ng
500 ng
1,000 ng
B
n.s.
*
Relative A3C mRNA expression
2.0
1.5
1.0
0.5
0.0
Uninfected
WT
LMP2A KO
AGS-EBV
C
*
*
*
Relative A3C mRNA expression
1.5
1
0.5
0
Mock
1
10
100
LMP2A (ng)
LMP2A-KO AGS-EBV

Figure 5